Inorg. Chem. **2003**, *42*, 5259–5266

Hydroxyl Radical Formation by O–O Bond Homolysis in Peroxynitrous Acid

Sergei V. Lymar,[†] Rafail F. Khairutdinov,[‡] and James K. Hurst*[,§]

Chemistry Departments, Brookhaven National Laboratory, Upton, New York 11973-5000, and Washington State University, Pullman, Washington 99164-4630, and Department of Chemistry & Biochemistry and Center for Nanosensor Technology, University of Alaska, Fairbanks, Alaska 99775-6160

Received March 18, 2003

Peroxynitrite decay in weakly alkaline media occurs by two concurrent sets of pathways which are distinguished by their reaction products. One set leads to net isomerization to NO_3^- and the other set to net decomposition to O_2 plus NO_2^-. At sufficiently high peroxynitrite concentrations, the decay half-time becomes concentration-independent and approaches a limiting value predicted by a mechanism in which reaction is initiated by unimolecular homolysis of the peroxo O–O bond, i.e., the following reaction: $ONOOH \rightarrow {}^{\bullet}OH + {}^{\bullet}NO_2$. This dynamical behavior excludes alternative postulated mechanisms that ascribe decomposition to bond rearrangement within bimolecular adducts. Nitrate and nitrite product distributions measured at very low peroxynitrite concentrations also correspond to predictions of the homolysis model, contrary to a recent report from another laboratory. Additionally, (1) the rate constant for the reaction $ONOO^- \rightarrow {}^{\bullet}NO + {}^{\bullet}O_2^-$, which is critical to the kinetic model, has been confirmed, (2) the apparent volume of activation for ONOOH decay ($\Delta V^{\ddagger} = 9.7 \pm 1.4$ cm^3/mol) has been shown to be independent of the concentration of added nitrite and identical to most other reported values, and (3) complex patterns of inhibition of O_2 formation by radical scavengers, which are impossible to rationalize by alternative proposed reaction schemes, are shown to be quantitatively in accord with the homolysis model. These observations resolve major disputes over experimental data existing in the literature; despite extensive investigation of these reactions, no verifiable experimental evidence has been advanced that contradicts the homolysis model.

Introduction

Interest in the chemical reactivity of peroxynitrous acid (ONOOH) has been rekindled by recognition that this powerful oxidant[1] could be formed in respiring tissues by radical coupling of $^{\bullet}O_2^-$ and $^{\bullet}NO$ and might thereby be a major contributor to diseases associated with oxidative stress and cellular mechanisms of host resistance to pathogenic organisms.[2] The oxidative behavior of ONOOH is highly unusual in the sense that many of its reactions are first-order in ONOOH and independent of the reductant concentration. Further, stoichiometric oxidation of the other reactant is never achieved in these reactions, with a significant portion of the product mixture being the ONOOH isomerization product, nitric acid. These properties indicate that oxidation requires rate-limiting conversion of ONOOH into secondary species that are the actual oxidants.[3]

The formation of radical intermediates in oxidations of simple aromatic compounds was evident 50 years ago from the appearance of diaryl compounds in the product mixtures,[4] and an early kinetic study established that decomposition to nitric acid was consistent with intermediary formation of $^{\bullet}OH$.[5] Hydroxyl radical was again suggested as the reactive species in a seminal paper that drew attention to the possible

* To whom correspondence should be addressed. E-mail: hurst@wsu.edu. Fax: (509) 335-8867. Voice: (509) 335-7848.
[†] Brookhaven National Laboratory.
[‡] University of Alaska.
[§] Washington State University.

(1) Koppenol, W. H.; Moreno, J. J.; Pryor, W. A.; Ischiropoulos, H.; Beckman, J. S. *Chem. Res. Toxicol*. **1992**, *5*, 834−842.
(2) Radi, R.; Peluffo, G.; Alvarez, M. N.; Naviliat, M.; Cayota, A. *Free Radical Biol. Med*. **2001**, *30*, 463−488. Stuehr, D.; Pou, S.; Rosen, G. M. *J. Biol. Chem*. **2001**, *276*, 14533−14536. Hurst, J. K.; Lymar, S. V. *Acc. Chem. Res*. **1999**, 32, 520−528. Beckman, J. S.; Koppenol, W. H. *Am. J. Physiol*. **1996**, *271*, C1424−1437. Pryor, W. A., Squadrito, G. L. *Am. J. Physiol*. **1995**, *268*, L699−L722.
(3) See, e.g.: Lymar, S. V.; Jiang, Q.; Hurst, J. K. *Biochemistry* **1996**, *35*, 7855−7861.
(4) Halfpenny, E.; Robinson, P. *J. Chem. Soc*. **1952**, 939−946.
(5) Mahoney, L. R. *J. Am. Chem. Soc*. **1970**, *92*, 5262−5263.

10.1021/ic030104l CCC: $25.00
Published on Web 07/25/2003

Scheme 1. Radical Pathways for Peroxynitrite Decay[a]

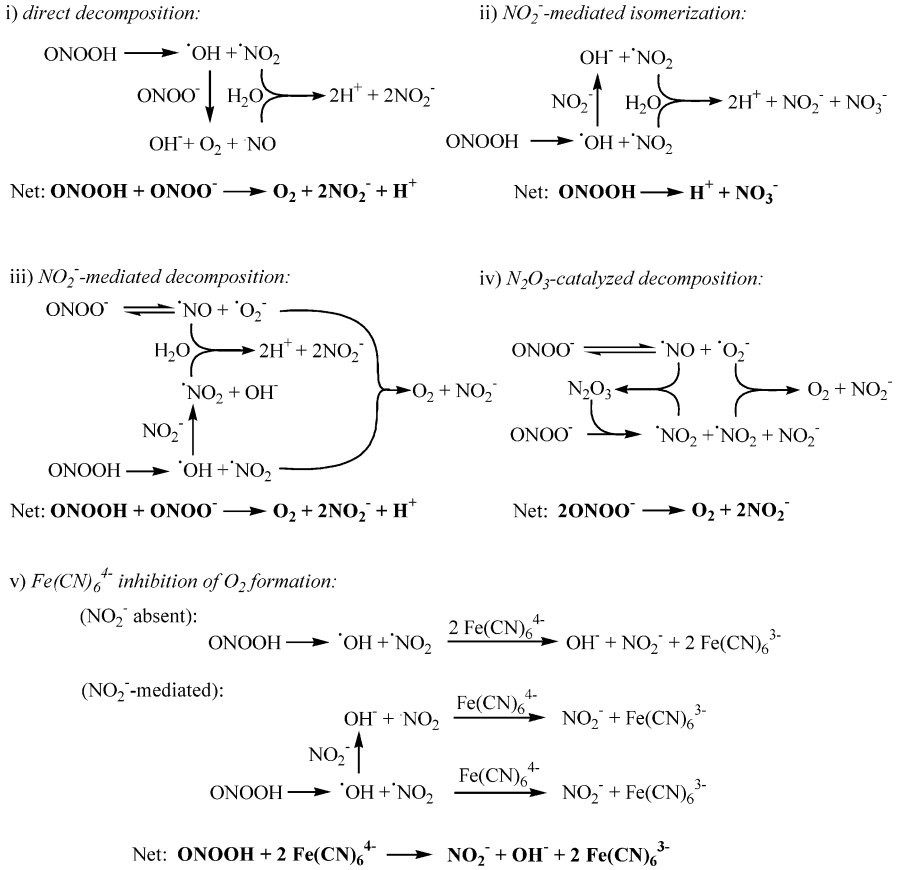

[a] Homolysis of the O−O bonds in ONOOH leads to initial formation of geminate {•NO_2, •OH} radical pairs, which then either (1) recombine to regenerate ONOOH, (2) isomerize within the solvent cage to give HNO_3, or (3) escape the cage as radicals to undergo bimolecular reactions with other solution components. For clarity, only those reactions that follow cage escape are shown, as the caged radicals are too short-lived to engage in reactions other than with themselves. Only ~28% of the total ONOOH undergoing decay leads to formation of these cage-separated radicals.[26,27] Although not shown, isomerization of ONOOH to $H^+ + NO_3^-$ is included in the mechanistic analysis of the data according to the homolysis model (as outlined in the Supporting Information).

biological significance of peroxynitrite.[6] However, this view was quickly abandoned when thermodynamic estimates suggested that the O−O bond in ONOOH was too strong to account for the rate of first-order oxidations by ONOOH; i.e., the measured rate constant for these reductant-independent oxidations was greater than that predicted for O−O bond homolysis.[1] An alternative mechanism was proposed which assigned the activation step to cis → trans isomerization of ONOOH with either the trans conformer or an unstable "transoid" intermediate being the reactive species. This model was widely adopted by the biomedical community at that time.

The thermodynamic analysis which formed the basis for rejection of O−O homolysis as the activation step was questioned by Merényi and Lind, who, by using a different set of premises, found that the calculated homolysis rate constant was consistent with measured values.[7] The ensuing debate over the relative merits of the two calculations[8] led us to seek resolution of the issue by examining whether intermediary formation of •OH and •NO_2 could account quantitatively for product distributions obtained from ONOOH decomposition.[9] In acidic media, ONOOH isomerizes quantitatively to HNO_3; in neutral to weakly alkaline media, a competing pathway involving decomposition to $O_2 + 2NO_2^-$ is expressed.[9−12] This behavior can be modeled by invoking a fairly complex set of reactions initiated by O−O homolysis; the important components comprising this set are displayed in Scheme 1 (pathways i−iv). Although these pathways are not entirely independent, each can prevail under certain reaction conditions. Because the rate constants for every elementary reaction in these pathways have been independently measured, it is possible in this case to calculate without

(6) Beckman, J. S.; Beckman, T. W.; Chen, J.; Marshall, P. A.; Freeman, B. A. *Proc. Natl. Acad. Sci U.S.A.* **1990**, *87*, 1620−1624.
(7) Merényi, G.; Lind, J. *Chem. Res. Toxicol*. **1997**, *10*, 1216−1220.
(8) Koppenol, W. H.; Kissner, R. *Chem. Res. Toxicol*. **1998**, *11*, 87−90. Merényi, G.; Lind, J.; Goldstein, S.; Czapski, G. *Chem. Res. Toxicol*. **1998**, *11*, 712−713. Very recently, the latter researchers have shown that calculation of the Gibb's energy of formation of ONOOH based upon the kinetically determined equilibrium constant for the reaction, ONOOH + $H_2O \rightleftarrows HNO_2 + H_2O_2$ (Merényi, G.; Lind, J.; Czapski, G.; Goldstein, S. *Inorg. Chem*. **2003**, *42*, 3796−3800) yields the same value as previously estimated by Merényi and Lind from the kinetically determined $ONOO^- \rightleftarrows {}^\bullet O_2^- + {}^\bullet NO$ equilibrium constant.[14] Thus, their calculations using thermodynamic cycles based upon two distinct reactions yield a self-consistent data set, thereby providing strong support for the O−O homolysis mechanism.
(9) Coddington, J. W.; Hurst, J. K.; Lymar, S. V. *J. Am. Chem. Soc*. **1999**, *121*, 2438−2443.
(10) Pfeiffer, S.; Gorren, A. C. F.; Schmidt, K.; Werner, E. R.; Hansert, B.; Bohle, D. S.; Mayer, B. *J. Biol. Chem*. **1997**, *272*, 3465−3470.
(11) Alvarez, B.; Denicola, A.; Radi, R. *Chem. Res. Toxicol*. **1995**, *8*, 859−864.
(12) Mark, G.; Korth, H.-G.; Schuchmann, H.-P.; von Sonntag, C. *J. Photochem. Photobiol., A: Chem.* **1996**, *101*, 89−103.

introducing any adjustable parameters the product distributions over a wide range of experimental conditions. We found that the model accurately predicted these distributions for all conditions reported in the literature and also accounted for some otherwise puzzling effects of added radical scavengers. We concluded that O−O homolysis is indeed the activation process in first-order reactions of ONOOH.

This conclusion has recently been challenged by Koppenol and Kissner, who have examined the product distributions over a wider range of experimental conditions.[13] Although their results are generally in agreement with earlier published data,[9,10] they find that, in alkaline solution at very low peroxynitrite concentrations, the measured yield of NO_2^- is less than predicted by the radical model. Indeed, if these data are correct, the radical model would have to be modified (in a way that is not obvious) or abandoned. Koppenol and co-workers have also challenged the model on a second point, namely, the rate constant used for the reaction step involving dissociation of peroxynitrite anion, i.e., $ONOO^- \rightarrow {}^\bullet NO + {}^\bullet O_2^-$. This rate constant, which is critical to the calculations, was measured indirectly by Merényi and Lind by observing the rate of formation of the nitroform anion, $C(NO_2)_3^-$, in alkaline solutions containing the $^\bullet O_2^-$ scavenger, tetranitromethane, $C(NO_2)_4$.[14] Koppenol and co-workers reported that $C(NO_2)_3^-$ formation was not inhibited when the medium also contained excess $^\bullet NO$, which is inconsistent with the mechanism proposed by Merényi and Lind.[15] However, in reexamining this experiment, Merényi, Goldstein, and coworkers found that under an atmosphere of $^\bullet NO$ the reaction of $ONOO^-$ with $C(NO_2)_4$ was completely inhibited, as the mechanism predicted.[16]

Since the whole issue of significant radical formation by ONOOH now rests upon resolving experimental discrepancies between laboratories, we have undertaken a careful reexamination of the points in dispute. Our findings, reported herein, remain totally consistent with the radical mechanism. Moreover, we present arguments on the basis of dynamical and stoichiometric evidence that eliminate from consideration an alternative mechanism proposed to account for ONOOH decomposition to O_2 and NO_2^-.[13]

Experimental Section

Materials. Alkaline peroxynitrite solutions were prepared by three different methods and stored frozen at −80 °C until used. Flow-mixing of $NaNO_2$ with acidic solutions of H_2O_2 followed by an alkaline quenching according to the explicit procedures of Saha et al. gave ∼100 mM $ONOO^-$ solutions that also contained ∼20 mM NO_2^-.[17] Ozonolysis of 0.1 M NaN_3 at pH 12 (NaOH) using a home-built ozonizer gave solutions that accumulated maximally 50−60 mM $ONOO^-$, which then declined upon further exposure to O_3, essentially as reported by Uppu et al.[18] To minimize residual N_3^- content,[18] ozonolysis was carried out until the $ONOO^-$ concentration had dropped to 25−30 mM; these solutions also contained ∼20 mM NO_2^-. Frozen solutions of tetramethylammonium peroxynitrite, synthesized according to Bohle et al.,[19] were kindly provided by Prof. Koppenol, ETH, Zurich. Decomposition of these peroxynitrite solutions during melting was minimized by addition of a small amount of NaOH to the frozen pellet before warming the sample. The solutions so obtained were ∼20 mM in $ONOO^-$ and contained ∼4 mM NO_2^-. To assess the short-term stabilities of the various preparations, decomposition rates of dilute $ONOO^-$ were briefly investigated at pH 12 and 23 °C. For all the preparations, decomposition was approximately linear in time over the span of 1−2 h; the rates of $ONOO^-$ loss in 5 mM samples prepared from $H_2O_2/NaNO_2$ and O_3/NaN_3 were ∼10%/h, and that in 0.4−0.8 mM $(CH_3)_4N(ONOO)$ was ∼20%/h. Addition of 0.67 mM diethylenetriaminepentaacetic acid did not affect the $(CH_3)_4N$-(ONOO) decomposition rate. As indicated in subsequent sections, all preparations gave equivalent results.

Methods. The kinetics of $C(NO_2)_3^-$ formation from $C(NO_2)_4$ were measured in an all-glass apparatus designed specifically to rigorously exclude O_2. This apparatus consisted of a round 50 mL mixing chamber connected via a 4-way V-bore stopcock to an optical cuvette.[20] The system was purged by percolating gases through the reaction medium; by rotating the stopcock 90°, the purging gas pressure could be used to drive the solution from the mixing chamber into the cuvette. The apparatus was also fitted with a double-septum antechamber through which anaerobic reactant solutions could be introduced using standard syringe-transfer techniques; the double-septum arrangement prevented adventitious O_2 from being carried into the reaction compartment during piercing of the septa. In a typical experiment, the reaction medium was first purged to obtain an atmosphere of N_2 or $^\bullet NO$, and then $ONOO^-$ and $C(NO_2)_4$ were added in that order. Immediately following the last addition, the optical cuvette was loaded and $C(NO_2)_3^-$ formation was monitored at 350 nm using a conventional diode array spectrophotometer (Hewlett-Packard 8452A). The time required to mount the cuvette was ∼30 s, so for the fastest reactions studied the first ∼30% of the reaction was not recorded. Dinitrogen trioxide was removed from commercial $^\bullet NO$ (AGA Specialty Gas, Cleveland, OH) by slowly passing the gas through two 0.5 M NaOH scrubbing towers, followed by a tower containing H_2O. The efficiencies of the scrubbers were checked by cycling $N_2/^\bullet NO/N_2$ through the reaction medium in the apparatus under conditions that duplicated those used for the kinetics experiments and then measuring the amount of accumulated NO_2^- using the standard Griess colorimetric assay.[21] Whereas accumulation of NO_2^- in the first NaOH scrubber was extensive (∼1 mM), the amounts in the second and third scrubbers were negligible and the amount in the reaction medium was below detectable limits (≲5 μM).

The yield of NO_2^- formed during alkaline decomposition of ONOOH was determined by measuring accumulated NO_2^- when known amounts of the peroxide were decomposed in anaerobic buffers prepared from NaH_2PO_4 (pH 4.5) or Na_2HPO_4 (pH 9.3). For each such analysis, serial additions of NO_2^- that had been standardized spectrophotometrically ($\epsilon_{354} = 24.7\ M^{-1}\ cm^{-1}$) were

(13) Kissner, R.; Koppenol. W. H. *J. Am. Chem. Soc*. **2002**, *124*, 234−239.
(14) Merényi, G.; Lind, J. *Chem. Res. Toxicol*. **1998**, *11*, 243−246.
(15) Nauser, T.; Merkofer, M.; Kissner, R.; Koppenol, W. H. *Chem. Res. Toxicol*. **2001**, *14*, 348−350.
(16) Goldstein, S.; Czapski, G.; Lind, J.; Merényi, G. *Chem. Res. Toxicol*. **2001**, *14*, 657−660.
(17) Saha, A.; Goldstein, S.; Cabelli, D.; Czapski, G. *Free Radical Biol. Med*. **1998**, *24*, 653−659.
(18) Uppu, R. M.; Squadrito, G. L.; Cueto, R.; Pryor, W. A. *Methods Enzymol*. **1996**, *269*, 311−321.
(19) Bohle, D. S.; Hansert, B.; Paulson, S. C.; Smith, B. D. *J. Am. Chem. Soc*. **1994**, *116*, 7423−7424.
(20) Zwickel, A. M., Ph.D. Dissertation, University of Chicago, 1959.
(21) Greenbert, A. E.; Conners, J. J.; Jenkins, D. *Standard Methods for the Examination of Water and Wastewater*, 15th ed.; American Public Health Association, United Book Press: Baltimore, MD, 1995; pp 4-83−4-84, 4-99.

Scheme 2. Radical Mechanism for Reaction between $ONOO^-$ and $C(NO_2)_4$

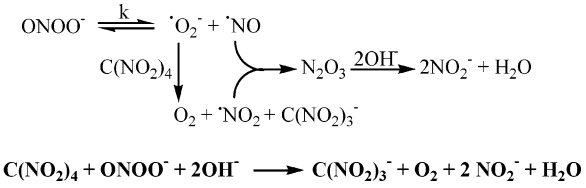

Net: $C(NO_2)_4 + ONOO^- + 2OH^- \longrightarrow C(NO_2)_3^- + O_2 + 2\,NO_2^- + H_2O$

made to the samples. This procedure allowed simultaneous determination of the molar extinction coefficient of the colorimetric product from the Griess reaction and the absorbance of the NO_2^- formed during peroxynitrite decay, thereby providing an internal check on the completeness of the analytical reactions. Reproducibilities were high, giving $\epsilon_{540} = (5.55 \pm 0.13) \times 10^4\ M^{-1}\ cm^{-1}$ for the 45 reaction product analyses made over the course of these studies. Samples were analyzed both manually in the laboratory and using a fully automated instrument at Anatek Laboratories (Moscow, ID). The automated system also performed nitrate analyses by incorporating an in-line Cd reduction coil which was 95% efficient in reducing NO_3^- to NO_2^-. Equivalent results were obtained for NO_2^- yields with the two methods. Additionally, the automated method allowed us to establish that the sole nitrogen-containing products of ONOOH decomposition were NO_2^- and NO_3^-; that is, the combined yields of these two ions were equal to within 3% when decompositions of individual solutions were carried out at pH 4 and pH 9. Fractional NO_2^- yields formed during alkaline decomposition of ONOOH were determined by dividing the difference in measured NO_2^- at these two pH values by the total added peroxynitrite.

The kinetics of peroxynitrite decay in weakly alkaline solutions were determined spectrophotometrically in the vicinity of the broad 302 nm absorption band ($\epsilon_{302} = 1670\ M^{-1}\ cm^{-1}$); when initial peroxynitrite concentrations were greater than ~2 mM, it was necessary to monitor the reaction at wavelengths to the red of the band maximum, even when using 0.1 cm path length cuvettes, to obtain accurate absorbance readings. These reactions were initiated by mixing concentrated buffer solutions with strongly alkaline solutions of $ONOO^-$. Pressure-dependent kinetics of ONOOH decomposition were measured using a Hi-Tech HPS-2000 stopped-flow spectrophotometer as previously described.[22]

Results and Discussion

Kinetics of the $ONOO^- \rightarrow {}^\bullet NO + {}^\bullet O_2^-$ Reaction. The rate constant for this reaction was first reported by Merényi and Lind,[14] who interpreted the enhanced rate of $C(NO_2)_3^-$ formation from $C(NO_2)_4$ in the presence of $ONOO^-$ in terms of the mechanism given in Scheme 2, where *k* denotes the rate-limiting step. As pointed out by Koppenol and co-workers,[15] if this mechanism were correct, one would expect the rate of $C(NO_2)_3^-$ formation to be suppressed in the presence of excess •NO, which would shift the competition for $^\bullet O_2^-$ in favor of the reverse $ONOO^-$-forming reaction at the expense of the reaction with $C(NO_2)_4$.

Experiments were performed under both the conditions initially reported by Merényi and Lind[14] and those subsequently reported by Koppenol and co-workers[15] and Goldstein and co-workers;[16] all three types of $ONOO^-$ preparations gave equivalent results.[23] A typical result is given in Figure 1. Under an N_2 atmosphere, formation of $C(NO_2)_3^-$ in the presence of limiting amounts of $ONOO^-$ could be quantitatively described by a rate law comprising rapid and slow concurrent first-order pathways. Under an •NO atmosphere, the rapid reaction was completely suppressed, but the slow reaction rate was unchanged; furthermore, its rate was identical within experimental uncertainty to the rate of alkaline hydrolysis of $C(NO_2)_4$ to $C(NO_2)_3^-$ measured in the absence of $ONOO^-$. The calculated rate constant for the rapid reaction was $0.012-0.016\ s^{-1}$, essentially identical to the value reported by Merényi and Lind[14] ($0.017\ s^{-1}$), and was independent of the medium alkalinity over the range pH 10−12. Overall, these data are in quantitative accord with results reported by the Merényi and Goldstein laboratories[14,16] but differ markedly from the results from the Koppenol laboratory,[15] which found no influence of •NO upon the reaction.

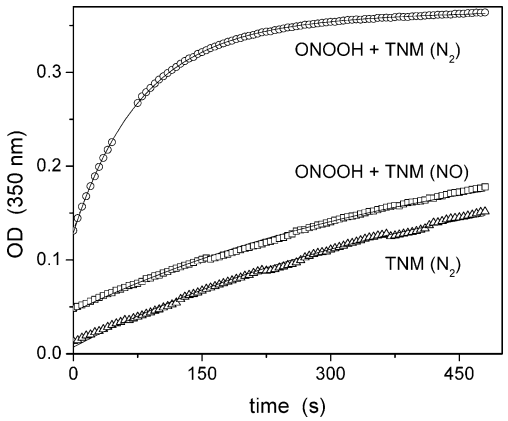

Figure 1. Nitroform anion formation kinetics in various media. Conditions: $[C(NO_2)_4]_0 \simeq 50\ \mu M$, pH 12 (NaOH), 22 °C. N_2 atmosphere, $[ONOO^-]_0 = 18\ \mu M$ (circles); •NO atmosphere, $[ONOO^-]_0 = 18\ \mu M$ (squares); N_2 atmosphere, $ONOO^-$ absent (triangles). The source material for this experiment was tetramethylammonium peroxynitrite. The lines are data fits for two concurrent first-order decay pathways with $\tau_1 = 86$ s and $\tau_2 = 440$ s (top) or a single first-order decay with $\tau = 440$ s (middle and bottom). TNM refers to $C(NO_2)_4$.

The rate constant for this reaction has now also been determined using an entirely different experimental design, namely, by measuring the rates of decay of radiolytically generated methyl viologen cation radicals ($^\bullet MV^+$) in the presence of $ONOO^-$;[24] like $C(NO_2)_4$, $^\bullet MV^+$ is a highly effective scavenger of $^\bullet O_2^-$.[25] The rate constant $k = 0.018\ s^{-1}$ at 25 °C calculated from these data is within experimental uncertainty identical to the value measured with $C(NO_2)_4$. Overall, these experiments vindicate the use of this rate constant in predictions based upon the radical reaction model (Scheme 1) and validate the calculated results.[9]

Product Yields from Peroxynitrite Decomposition. Kissner and Koppenol have reported that the yields of O_2

(22) Coddington, J. W.; Wherland, S.; Hurst, J. K. *Inorg. Chem.* **2001**, *40*, 528−532.

(23) The use of the "Zwickel" reaction vessel[20] was prompted by informal discussions with Professors Koppenol, Czapski, and Goldstein concerning the possibility that adventitious O_2 might contribute to the reported experimental discrepancies. These earlier studies were made using stopped-flow instrumentation,[14−16] which is vulnerable to contamination by atmospheric gases; in contrast the glass assembly used in this study is leak-proof when properly purged.

(24) Lymar, S. V.; Poskrebyshev, G. Manuscript submitted for publication.

(25) Levy, G.; Ebbesen, T. W. *J. Phys. Chem.* **1983**, *87*, 829−832.

and NO_2^- obtained from decomposition of peroxynitrite at low concentrations in alkaline solutions are significantly less than predicted by the radical model.[13] Upon reinvestigating this point using peroxynitrite solutions prepared by reaction between H_2O_2 and $NaNO_2$, by N_3^- ozonolysis, and in the Koppenol laboratory from solid tetramethylammonium peroxynitrite, we find no discrepancy between experimentally determined and predicted yields. In these studies, several different $H_2O_2-NaNO_2$ preparations were used, all of which gave equivalent results; NO_2^- yields measured in samples that had been stored at −80 °C for up to 1 year were unchanged from yields obtained on the same samples shortly after preparation, indicating that long-term storage had no effect upon the reaction stoichiometry, as should be expected. The total amounts of NO_2^- and NO_3^- present in product solutions that had decayed at pH 4.5 and 9.3 were identical, indicating that no other nitrogen-containing species were formed. Relevant data from both laboratories are displayed in Figure 2a; also shown (Figure 2b) are results of calculations based upon the radical mechanism (Scheme 1) that predict that the fractional yields will be insensitive to pH in the measured region but increase slowly with increasing peroxynitrite concentrations toward an asymptotic limit of ∼85%. Also, at 1.2 mM total peroxynitrite, the measured nitrite yield was 69%, in accord with predictions based upon Scheme 1 (Figure 2b) and with our earlier results based upon O_2 measurements.[9] The NO_2^- yields were independent of ionic strength over the measured phosphate concentration range of 50−500 mM; very similar yields of 42% at 25 μM peroxynitrite and 40% at 50 μM peroxynitrite were obtained in 50 mM NH_3/NH_4NO_3 buffer, pH 9.3. Our data are therefore quantitatively consistent with predictions based upon the radical mechanism over the entire experimental range that has been reported. They are also consistent with recent experimentally determined yields of secondary oxidants generated by ONOOH decomposition.[26−28]

Pressure Dependence of Peroxynitrite Reactions. Homolysis of ONOOH to two neutral fragments is expected to give rise to a significant increase in the molar volume of the transition state ($\Delta V^{\ddagger}$), so that reactions initiated by O−O homolysis will be inhibited at high pressures. The Koppenol laboratory originally reported $\Delta V^{\ddagger} = 1.7$ cm^3/mol for ONOOH decomposition, from which they argued that the reaction did not occur by homolysis;[29] they have subsequently revised this number upward.[30] Reinvestigations by other groups[22,31] have placed $\Delta V^{\ddagger}$ at ≃ 10 cm^3/mol for this reaction and for indirect oxidations (e.g., of $Fe(CN)_6^{4-}$) by ONOOH. In contrast, direct bimolecular reactions involving ONOOH exhibit negative values for $\Delta V^{\ddagger}$ which are dependent upon the reductant identities.[22] Relevant data are displayed in Figure 3; as discussed in the original papers,[22,31] the larger $\Delta V^{\ddagger}$ value is fully consistent with O−O bond homolysis being the ONOOH activation step.

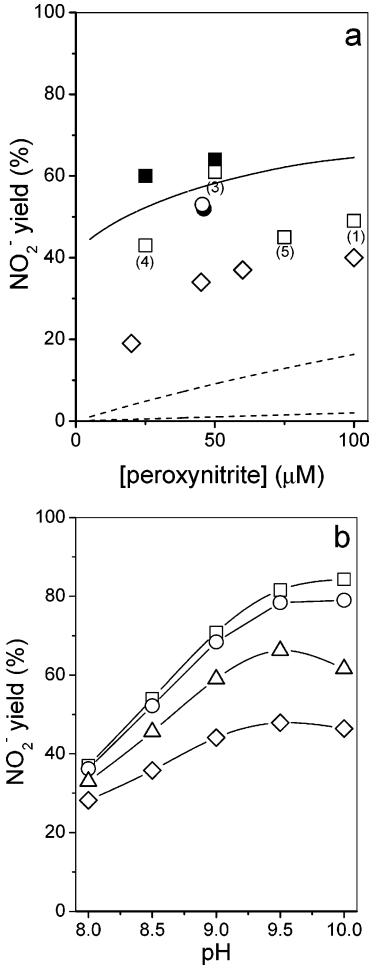

Figure 2. Nitrite yields from peroxynitrite decay in alkaline solutions. Panel a: measured yields at 22 °C in 0.1 M disodium hydrogen phosphate, pH 9.3. Solid squares (automated) and open squares (manual) indicate Griess analyses of reagent prepared by reaction between H_2O_2 and $NaNO_2$ (given in parentheses are the numbers of individual determinations made using separate preparations, with an estimated error of ±10%). The solid circle indicates manual Griess analysis of reagent prepared by azide ozonolysis,[18] and the open circle indicates manual Griess analysis of a solution of tetramethylammonium peroxynitrite. The open diamonds represent data reported by Kissner and Koppenol for pH 9.0.[13] The solid line presents the calculated yield at pH 9.3 for these conditions on the basis of the radical mechanism in Scheme 1. Dashed lines give calculated yields for the bimolecular pathway at pH 9.0 according to Scheme 3 with $K_a = 1.6 \times 10^{-7}$ M, $k_i = 1.2$ s^{-1}, and $K_A k_d = 2.5 \times 10^3$ M^{-1} s^{-1} (upper line) or $K_A k_d = 2.5 \times 10^2$ M^{-1} s^{-1} (lower line). Panel b: pH and concentration dependence for nitrite yields in this region, as predicted by the radical mechanism according to Scheme 1. Peroxynitrite concentrations are the following: 10 μM (diamonds); 100 μM (triangles); 500 μM (circles); 1000 μM (squares).

In our earlier investigation of the pressure dependence of ONOOH decomposition we reported an apparent dependence of $\Delta V^{\ddagger}$ upon the NO_2^- concentration.[22] This effect cannot be accommodated by the simple radical mechanism given in Scheme 1. Reinvestigation of this reaction over a wider range of conditions has shown that the effect was artifactual and that $\Delta V^{\ddagger}$ is independent of $[NO_2^-]$ in accord with the model (Figure 3 inset).

(26) Gerasimov, O. V.; Lymar, S. V. *Inorg. Chem*. **1999**, *38*, 4317−4321.
(27) Hodges, G. R.; Ingold, K. U. *J. Am. Chem. Soc*. **1999**, *121*, 10695−10701.
(28) Nakao, L. S.; Ouchi, D.; Augusto, O. *Chem. Res. Toxicol*. **1999**, *12*, 1010−1018.
(29) Kissner, R.; Nauser, T.; Bugnon, P.; Lye, P. G.; Koppenol, W. H. *Chem. Res. Toxicol*. **1997**, *10*, 1285−1292.
(30) $\Delta V^{\ddagger} = 6-7$ cm^3/mol (W. H. Koppenol, personal communication).
(31) Goldstein, S.; Meyerstein, D.; van Eldik, R.; Czapski, G. *J. Phys. Chem. A* **1999**, *103*, 7114−7118.

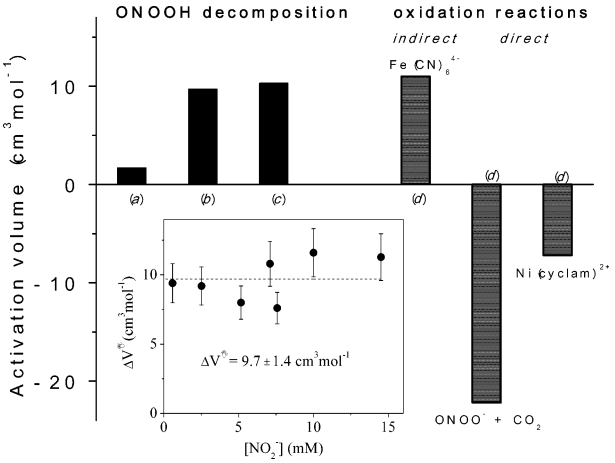

Figure 3. Pressure dependence of peroxynitrite reactions. Data are from the following: (a) ref 29; (b) this work; (c) ref 31; (d) ref 22. The inset gives the dependence of $\Delta V^{\ddagger}$ upon $[NO_2^-]$ measured in this work for decomposition of 0.35 mM ONOOH in 0.15 M sodium phosphate, pH 4.5, and 20 °C.

Inadequacies of Other Proposed Reaction Mechanisms. At pH 8−11, where decomposition into NO_2^- and O_2 is the dominant pathway, the kinetics of peroxynitrite decay exhibit nonexponential behavior and pronounced medium effects[29] whose origins have not been conclusively identified.[32] Consequently, full mechanistic analysis of the decay kinetic profiles is rendered equivocal. Although significant, the deviations from exponentiality are not dramatic and the experimentally determined peroxynitrite half-life, $t_{1/2}$, gives a useful quantitative parameter, which can be more conventionally expressed as the apparent rate constant, $k_{app} = \ln 2/t_{1/2}$, and used for comparing predictions of different models with the kinetic data. The radical mechanism clearly predicts that at high concentrations the apparent rate constant for decay will become independent of the initial peroxynitrite concentration (C_0). As required by this model, k_{app} became independent of C_0 at sufficiently high peroxynitrite concentrations (Figure 4). Furthermore, the model fairly accurately gives the limiting value for k_{app}. Under the chosen experimental conditions, medium effects were negligible.[32] Specifically, k_{app} was independent of the buffer identity (phosphate vs ammonium) and concentration over a severalfold range (Figure 4). No evidence of metal ion catalysis of $ONOO^-$ decay was found; addition of 1 mM of the chelators diethylenetriaminepentaacetic acid or bathocuproin disulfonate to the phosphate buffers, passage of buffer solutions down Chelex-100 cation exchange columns, and use of purified water and buffer salts from various sources had no effect on the decay profiles.

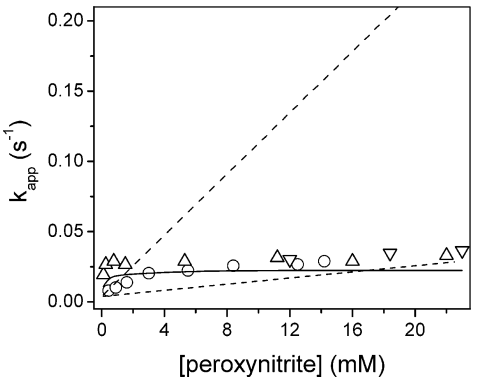

Figure 4. Apparent rate constants (as defined in the text) for peroxynitrite decay in various media. Conditions: 0.06 M disodium hydrogen phosphate, pH 9.3 (circles); 0.012 M disodium hydrogen phosphate, pH 9.3 (inverted triangles); 0.05 M ammonia/ammonium nitrate, pH 9.4 (upright triangles); all reactions at 22 °C. The solid line shows the dependence predicted by the radical mechanism according to Scheme 1; dashed lines show the dependence predicted for reaction according to Scheme 3 using K_a and k_i given in Figure 2a and $K_A k_d = 2.5 \times 10^3\ M^{-1}\ s^{-1}$ (upper line) or $K_A k_d = 2.5 \times 10^2\ M^{-1}\ s^{-1}$ (lower line).

Scheme 3. Bimolecular Pathway for Peroxynitrite Decay[13]

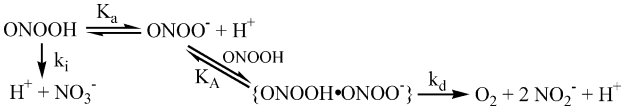

Koppenol and co-workers have proposed that decomposition of peroxynitrite to O_2 and NO_2^- proceeds through a second-order reaction involving association of ONOOH and $ONOO^-$ to form a cyclic dimer that subsequently undergoes concerted bond rearrangement (Scheme 3) ;[13] this mechanism is generally accepted as one of the bimolecular pathways for decomposition of organic and inorganic peroxides.[33] However, unlike these peroxides, ONOOH also decays by concurrent isomerization to nitric acid. Consequently, the rate law predicted by Scheme 3 for peroxynitrite decay is more complex than the simple second-order rate laws that describe decomposition of other peroxides. The analytical solution to the rate law for the decay reaction given in Scheme 3 is

$$C_t = C_0 \frac{\exp(-k_1 t)}{1 + P\{1 - \exp(-k_1 t)\}}$$

where $C_0 = [ONOO^-]_0 + [ONOOH]_0$ is the initial concentration of peroxynitrite not bound in the dimer, C_t is the

(32) The radical model predicts that high levels of phosphate ions can be rate-retarding under the experimental conditions. This follows because N_2O_3, formed during peroxynitrite decomposition, reacts rapidly with $ONOO^-$, setting up a catalytic cycle for further decomposition (Scheme 1, pathway iv). The magnitude of the contribution of pathway iv to peroxynitrite decay is determined by the relative rates of reaction of N_2O_3 with peroxynitrite anion and solvent, i.e., the following reaction: $N_2O_3 + H_2O \rightarrow 2H^+ + 2NO_2^-$. Under highly alkaline conditions, hydrolysis of N_2O_3 by OH^- will be the dominant reaction.[34] Thus, pathway iv will contribute to peroxynitrite decay only in weakly alkaline solutions (pH ≃ 7−12). Earlier work on N_2O_3 nitrosation reactions[35,36] has indicated that N_2O_3 hydrolysis could be catalyzed by phosphate. At sufficiently high concentrations, phosphate will therefore effectively remove N_2O_3 via hydrolysis, decreasing N_2O_3-catalyzed peroxynitrite decay via pathway iv and thereby decreasing the overall decay rate in weakly alkaline media. Because the rate constant for reaction between phosphate and N_2O_3 is not known at pH 9, this reaction was not included in the lifetime calculations. This omission appears justified on the basis that the experimentally determined values were insensitive to both phosphate buffer concentration at low ionic strengths and the identity of the buffer (Figure 4).

(33) Koubek, E.; Levey, G.; Edwards, J. O. *Inorg. Chem.* **1964**, *3*, 1331−1332. Ball, R. E.; Edwards, J. O. *J. Am. Chem. Soc.* **1956**, *78*, 1125−1129. Goodman, J. F.; Robson, P.; Wilson, E. R. *Trans. Faraday Soc.* **1962**, *58*, 1846−1851. Goodman, J. F.; Robson, P. *Trans. Faraday Soc.* **1963**, *59*, 2871−2875. Ball, R. E.; Edwards, J. O.; Haggett, M. L.; Jones, P. *J. Am. Chem. Soc.* **1967**, *89*, 2331−2333.
(34) Treinin, A.; Hayon, E. *J. Am. Chem. Soc.* **1970**, *92*, 5821−5828.
(35) Goldstein, S.; Czapski, G. *J. Am. Chem. Soc.* **1996**, *118*, 3419−3425.
(36) Lewis, R. S.; Tannenbaum, S.; Deen, W. M. *J. Am. Chem. Soc.* **1995**, *117*, 3933−3939.

corresponding current concentration, and $P = 2k_2C_0/k_1$ is a dimensionless parameter that describes the partitioning between the bimolecular decomposition and unimolecular decay pathways. In this equation, k_1 is the rate constant for ONOOH isomerization under the prevailing medium conditions, given by $k_1 = k_i/(1+ K_a/[H^+])$, where k_i is the pH-independent isomerization rate constant and K_a is the ONOOH acid dissociation constant; similarly, $k_2 = K_A k_d/\{(1 + K_a/[H^+])(1 + [H^+]/K_a)\}$, where k_d is the rate constant for decomposition of the dimer formed between ONOOH and $ONOO^-$ and K_A is the dimer formation constant. From the integrated form of the rate law, one obtains

$$k_{app} = \frac{\ln 2}{t_{1/2}} = k_1 \frac{\ln 2}{\ln(2 + P) - \ln(1 + P)}$$

for the apparent rate constant of peroxynitrite decay and $Y_{nitrite} = 1 - \ln(1 + P)/P$, for the nitrite yield, defined as $Y_{nitrite} = [NO_2^-]_\infty/C_0$.

Although there are four fundamental constants in this model, two of them (k_i and K_a) are well established from independent studies; furthermore, the other two (k_d and K_A) are mutually dependent in the sense that only their product ($K_A k_d$) determines k_2 and, therefore, P, which in turn determines the magnitude of NO_2^- yields and the concentration dependence of the peroxynitrite decay half-lives. As the following considerations will show, there exists no value for $K_A k_d$ that can simultaneously account (even approximately) for NO_2^- yields at low peroxynitrite concentrations and decay rates at high peroxynitrite concentrations. Consequently, one must conclude that the decay mechanism presented in Scheme 3 is in irreconcilable contradiction with the data and, thus, is incorrect. The apparent rate constant for peroxynitrite decay at high reactant concentrations can be approximated (although rather poorly) by the Scheme 3 reaction model when $K_A k_d = 2.5 \times 10^2\ M^{-1}\ s^{-1}$ (Figure 4, lower dashed line). However, using these constants, the NO_2^- yields at low reactant concentrations are calculated to be negligible, in marked contrast to measured yields (Figure 2a, lower dashed line). Even modestly increasing $K_A k_d$ to $2.5 \times 10^3\ M^{-1}\ s^{-1}$ in an attempt to improve the "fit" to the yield data (Figure 2a, upper dashed line) generates a very strong concentration dependence for the decay rate at high peroxynitrite concentrations (Figure 4, upper dashed trace) that is at odds with the rate data. When proposing parameters for Scheme 3, Koppenol and co-workers indicated that these parameters "may be refined".[13] However, it is evident that no refinement is possible, as no single combination of K_A and k_d will be found that can satisfy both sets of data for the yields and the rates in Figures 2 and 4. In contrast, the radical model presented in Scheme 1 (for which there are no adjustable parameters) adequately accounts for both rate and yield data over the entire experimentally accessible range (Figures 2a and 4, solid lines).

Finally, we note that bimolecular decomposition mechanisms such as that shown in Scheme 3 also cannot explain the complex effects of added redox reagents upon the product distributions, although these effects are quantitatively predicted by the radical mechanism from known, i.e., independently measured, rate constants.[9] Specifically, added NO_2^- selectively inhibits O_2 production from peroxynitrite decomposition in neutral but not in alkaline solutions (Figure 5). Organic radical scavengers also inhibit peroxynitrite decomposition; this inhibition is reversed in alkaline solutions by addition of NO_2^- (Figure 6). However, inhibition of decomposition by $Fe(CN)_6^{4-}$ is not reversed by NO_2^- (Figure 6). These effects can be explained by the radical mechanism (Scheme 1) as follows: in neutral media, NO_2^- competes with $ONOO^-$ for $^\bullet OH$ (pathways i and ii), generating NO_3^- instead of $O_2 + NO_2^-$; under more alkaline conditions (pathway iii), the $^\bullet NO_2$ formed from reaction between NO_2^- and $^\bullet OH$ reacts with $^\bullet NO$ or $^\bullet O_2^-$ generated by $ONOO^-$ dissociation rather than another $^\bullet NO_2$. The immediate product of the $^\bullet NO + {}^\bullet NO_2$ reaction is N_2O_3, a catalyst for the O_2-forming pathway iv. Added organic radical scavengers react with $^\bullet OH$ formed by ONOOH peroxo bond homolysis, reducing O_2 yields; NO_2^- effectively competes with these scavengers for $^\bullet OH$, restoring the yields (pathway iii). Unlike the organic reductants, $Fe(CN)_6^{4-}$ reacts rapidly with $^\bullet NO_2$ as well as $^\bullet OH$ (pathway v), so that its inhibition of O_2 formation cannot be reversed by addition of NO_2^-. At the concentration levels used, $Fe(CN)_6^{4-}$ does not react directly with peroxynitrite.[26]

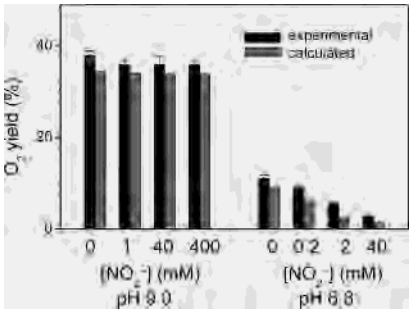

Figure 5. Nitrite dependencies of O_2 yields.[9] Conditions: 0.55 mM peroxynitrite decomposed in 0.3 M sodium phosphate at 21 °C. Calculated yields are based upon the radical mechanism presented in Scheme 1. Predicted NO_2^- yields are twice the measured O_2 yields. The bimolecular mechanism of Scheme 3 predicts nitrite-independent O_2 yields of 24% and 17% for pH 9.0 and 6.8, respectively, under these conditions.

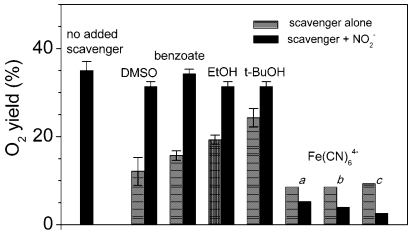

Figure 6. Influence of radical scavengers upon O_2 yields.[9] Reaction conditions: all reactions at pH 9.0; other conditions as in Figure 5. When present, organic scavenger and NO_2^- concentrations were 1.0 mM, except that, with t-BuOH, $[NO_2^-] = 0.5$ mM when added. For organic scavengers, both black and shaded bars are experimental. The data for $Fe(CN)_6^{4-}$ quenching provide comparison between experimental (shaded bar) and calculated (black bar) values on the basis of Scheme 1. For these reactions $[Fe(CN)_6^{4-}] = 0.5$ mM, with $[NO_2^-] = 0$ (set a), 0.5 mM (set b), or 5.0 mM (set c).

Acknowledgment. The authors are grateful to John W. Coddington of Anatek Laboratories (Moscow, ID) for

conducting the automated NO_2^- and NO_3^- concentration analyses reported in this paper and to Professor Willem Koppenol, Eidgenössische Technische Hochschule, Zurich, for providing frozen solutions of tetramethylammonium peroxynitrite. Funding for this research was provided by the National Institutes of Health under Grant AI-15834 (to J.K.H.). Research at Brookhaven National Laboratory was carried out under the auspices of the U.S. Department of Energy under Contract DE-AC02-98CH10886 from the Division of Chemical Sciences, Office of Basic Energy Sciences, and EMPS Grant No. 73824 (to S.V.L.) from the Office of Environmental Management.

Supporting Information Available: Derivation of the rate law for Scheme 3 and a table of rate constants for elementary steps used in numerical simulations based upon Scheme 1. This information is available free of charge via the Internet at http://pubs.acs.org.

IC030104L